Chapter 7

Surface Integrity Characterization of Ground Surface using Magnetic Barkhausen Noise Technique

7 Introduction

Grinding is often classified as a thermo-mechanical process rather than a mechano-thermal process due to the significant proportion of energy conversion occurring, ranging from 60% to 85% within the grinding process. Conversely, in conventional machining processes such as turning and milling, only approximately 20% of the generated heat is transferred to the workpiece through conduction [8]. High heat conduction into the workpiece during the grinding process gives rise to high temperature, which impairs the ground surface's surface integrity in the form of thermal damage, rehardening, generation of tensile residual stresses, and micro-cracks [100]. These thermal damages on the ground surface restrict the grinding process's ability to achieve the desired production rate. Hence, reliable, and faultless thermal damage detection is important to achieve the desired production rate without sacrificing product quality. Currently, the researcher frequently uses conventional measurement techniques such as metallographic inspection, SEM, AFM, energy-dispersive X-ray spectroscopy (EDX), X-ray diffraction (XRD), and hardness measurement to assess thermal damage. However, these techniques being time-consuming, costly, and laboratory-based, cannot be used for online monitoring of the thermal damage on the ground surface [240]. Moreover, the available literature cited in Chapter 2 revealed that in the last decade, Magnetic Barkhausen noise (MBN) and hysteresis loop (HL) techniques emerged as a potential non-destructive tool to characterize surface integrity of the machined component [101].

The present chapter explores the application of novel non-destructive techniques like MBN and HL in the grinding process to characterize the surface integrity and qualitatively assess the thermal damage of AISI D2 tool steel under dry, wet, MQL and UVAMQL grindings modes. The experiment was conducted at an extreme downfeed of 40 μm with six environments: dry, flood, SO, SO+DW emulsion, Al_2O_3 NFs (0.5% wt.) and Al_2O_3 NFs (1% wt.). UVAMQL grinding in combination with MBN, or HL may lead to efficient grinding with a fast characterization of ground samples, reducing the product's cycle time. The effect of machining heat on the ground surface was examined in terms of the ground surface, grinding temperature and microhardness. Besides, MBN and HL outcomes like root mean square (RMS), Peak, permeability, coercivity, and MBN and HL envelopes were correlated with surface property, i.e., microhardness under different environments.

7.1 Experimental procedure

Details of the material used, its chemical compositions, thermo-mechanical properties, and heat treatment procedure are detailed in Chapter 3, section 3. The grinding setup used, abrasive wheel designation, and dressing setting are described in Chapter 3, section 3.1. The workpiece dimension and grinding parameters used to perform the final experiments are the same as those used in Chapter 6.

7.1.1 Magnetic Barkhausen noise setup

The MBN signal and hysteresis loop measurements were carried out using a commercially available MAGSTAR system supplied by Technofour, India. The measurement system consists of a probe with a magnetizing yoke to generate a magnetic field in the ground sample. The magnetic response of the work material was collected using a pick-up coil placed at the centre of the probe. Magstar V3 software was employed to set various MBN parameters from the generated signal. The ground sample was cleaned with acetone to

remove any dirt and dust from the surface, which can affect the sample's magnetization. MBN test was performed at three different locations in the sliding direction of grinding. Figure 7.1 shows the various

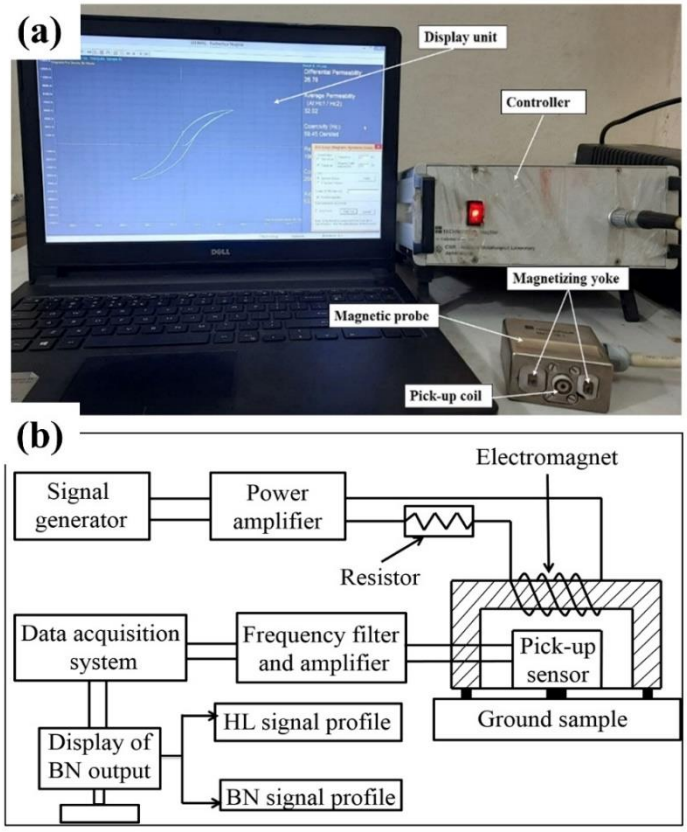

Figure 7.1 (a) Measurement arrangement of MBN analyzer, (b) Block diagram of MBN system for ground sample

components of the MBN analyzer and block diagram of the MBN system. The MBN and HL testing parameters are listed in Table 7.1. The MBN analysis applies the current to the magnetizing yoke as sinusoidal waveforms (refer to Figure 7.2 (c)). This excitation current generates a primary magnetic field in the test sample, as shown in Figure 7.2 (a). At OFF time, this supplied current was shortly turn-out of a large electromotive force, which induced an eddy current in the sample. This results in magnetic domain wall nucleation, translation, and rotation toward eddy current. Magnetic domain wall displacement is disturbed due to thermal damage effected on the grain boundaries and crystal planes.

Table 7.1 MBN testing parameters and their levels

MBN parameters	No. of cycle	3
	Magnetizing frequency	25 Hz
	Magnetic field intensity	200, 300, 400 and 500 Oe
	Response output	RMS, Peak, MBN loop
HL parameters	Wave from	Sine wave
	Magnetizing frequency	0.05, 0.1, 0.15, and 0.2 Hz
	Magnetic field intensity	450 Oe
	Response output	Permeability, Coercivity, HL loop

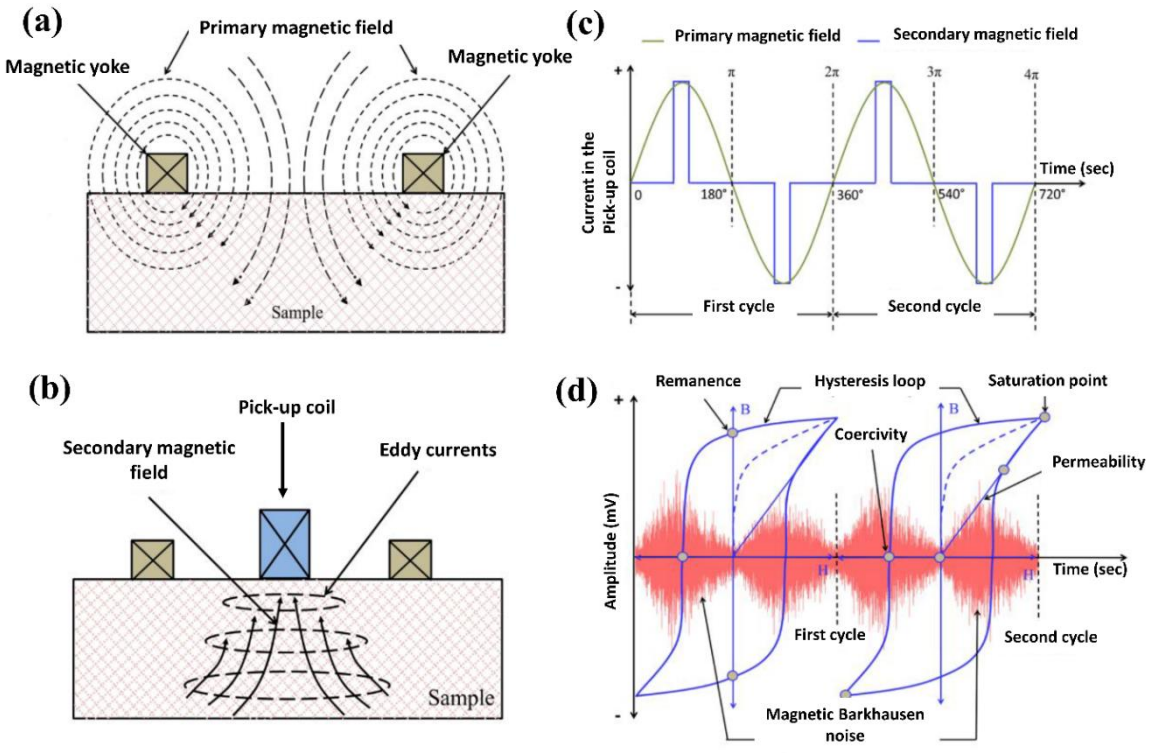

Figure 7.2 (a) Primary magnetic field produced by the magnetic yoke, (b) Secondary magnetic field captured by a pickup coil, (c) Current supplied in the form of a sinusoidal wave, (d) Formation of MBN signal and HL envelope

Subsequently, this eddy current develops a secondary magnetic field, which is collected using a pick-up coil placed at the centre of the probe, as shown in Figure 7.2 (b). The MBN signal was recorded for three cycles, and each cycle had two bursts corresponding to the magnetization and demagnetization of the test sample. The HL envelope produces against energy loss in one complete cycle of magnetization and demagnetization, as shown in Figure 7.2 (d).

7.2 Results and discussion

7.2.1 Effect of thermal damage on ground surface under different environments

The grinding process increases temperatures over the workpiece by the rubbing, ploughing, and shearing action of the grinding wheel that has randomly oriented abrasive grains with a high negative rake angle. Overheating during grinding results in thermal damage to the surface in the form of oxidation, burning, and the creation of microcracks.

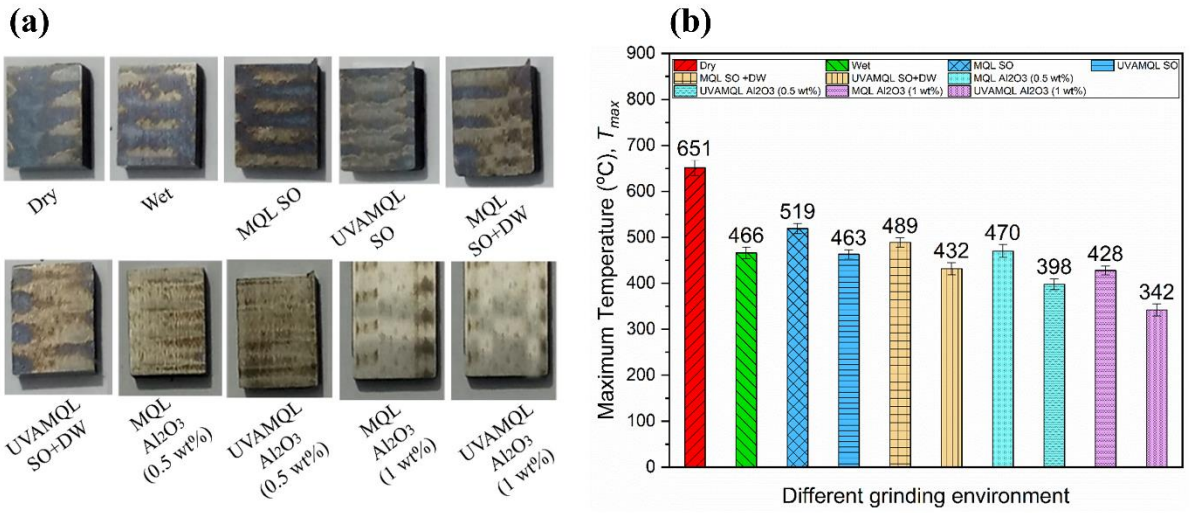

Figure 7.3 (a) Thermally damaged ground samples, (b) Variation in grinding temperature under different environments.

Figure 7.3 (a) and (b) show the thermal damage inflicted on ground samples and measured grinding temperature value under different grinding environments. Thus, it is clearly indicated from Figure 7.3 (a) and (b) that a higher temperature (651°C) has more thermal damage, and a lower temperature (342°C) has very low or negligible thermal damage. A lower grinding temperature was obtained at a higher downfeed under UVAMQL with Al_2O_3 NFs (1 wt.%), as revealed in Figure 7.3 (b). This is because the ultrasonic vibration reduces the contact time between abrasive grits and workpiece along with that Al_2O_3 NFs have extracted the maximum amount of heat from the grinding zone. During the grinding process using NFs, Al_2O_3 NPs produced a rolling effect than the sliding action between the grinding wheel and workpiece, resulting in lower friction force and low heat penetration in the ground sample. As seen in Figure 7.3 (a), dry grinding caused severe grinding burns on the ground sample because cooling and lubricating conditions were absent. Similarly, a high surface roughness value was obtained in the dry mode, as mentioned in Chapter 5 (section 5.2.4). It was mainly due to generating more heat, which produced blunt edges of abrasive grits, causing more rubbing and ploughing than shearing phenomena. Clearly, a substantial quantity of heat permeated the sample after dry grinding. Further, under MQL grinding with SO has poor surface quality due to its thermo-physical properties (refer to Figure 6.7).

7.2.2 Effect of thermal damage on microhardness under different environments

Microhardness is the hardness of a material as examined by pressing an indenter such as a Vickers or Knoop indenter into the material's surface under a 10 to 1000 gm load. The microhardness measurement makes it possible to quickly evaluate the microstructural change that has occurred in the ground's surfaces. Generally, the microhardness of a material is directly dependent on its microstructural features, which can include plastic

deformation, phase transformation, grain boundaries, grain refinements, etc. As part of the experimental analysis, microhardness measurements were performed on the ground sample's surface layer to analyse how the grinding environments influence the final surface layer hardness, which is frequently observed for ground surfaces. This study conducted a microhardness measurement on a cross-section of the ground's surface. The load magnitude was set to 100 gm per 10 s dwell time for analyzing the microhardness.

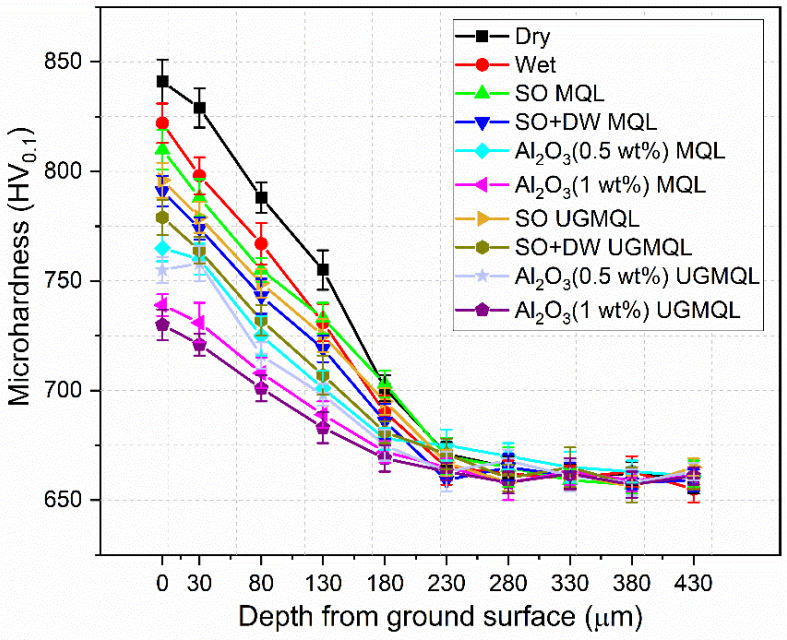

Figure 7.4 Microhardness under various grinding modes

Figure 7.4 represents the change in microhardness as a function along with a depth from the ground surface using the alumina grinding wheel under dry, wet, SO MQL, SO+DW MQL, Al_2O_3 (0.5 wt.%) MQL, Al_2O_3 (1 wt.%) MQL, SO UVAMQL, SO+DW UVAMQL, Al_2O_3 (0.5 wt.%) UVAMQL, Al_2O_3 (1 wt.%) UVAMQL grinding. In the grinding, work material goes through several abrasive grits action. Hence, the ground surface is plastically deformed and thermally damaged in the shearing direction, resulting in the hardness of the ground surface being much higher than the base metal. Further, it was exponentially diminishing with increasing subsurface depth up to base metal hardness. The reason is to

minimize the work-hardening effect along with subsurface depth. Researchers also reported that hardness profile exponentially decreases along with depth from ground surface owing to a reduction in thermal softening effect [284].

Figure 7.4 also showed that maximum hardness was observed in dry grinding as compared to other environments. It was mainly due to high heat penetration in the ground surface, which induced large grain refinement in the plastic deformation region. The small grain is improved strength of the plastically deformed layer, providing higher hardness on the ground surface and subsurface of the sample. Meyers and Chawla [285] explained the fundamental relation of grain size and hardness with the help of the Hall-Petch effect. Compared to a dry environment, a relatively lower microhardness value was observed in wet, MQL, and UVAMQL environments because of lower heat penetration in the ground sample. This may be attributed to the existence of strong anti-friction lubricating tribo-film, which provided effective lubrication in the grinding wheel and work material interface. This was reducing heat penetration in the ground surface at lower downfeed for the short grinding duration. The grinding with Al_2O_3 (1 wt.%) NFs lubricant under the UVAMQL environment produced the lowest microhardness variation, as illustrated in Figure 7.4. This happened due to the characteristics of separability by ultrasonic vibration, the rolling effect of NPs and a uniform protective lubricating boundary layer between the grinding wheel and workpiece. Consequently, this reduced the friction force and heat penetration in the ground surface, contributing to a more consistent lower microhardness value across the ground. Similarly, Wang et al. [278] observed the rolling effect of Al_2O_3 NPs on the ground surface during the grinding of the GH4169 workpiece, resulting in anti-friction and anti-wear.

7.2.3 Analysis of ground sample by magnetic BN parameters under different environments

Process variables in grinding, such as downfeed, table feed rate, and grinding environments, are critical in producing thermal damage incurred to the machined surface (discussed in Chapter 5 and 6). Grinding burns on the ground surface, which are thermal damage, change the ferromagnetic material's domain wall movement when an external magnetic field is applied and, as a result, significantly impact BN signal emission. Figure 7.5 (a-b) indicates the effect of grinding environments on BN signal, i.e., RMS and peak under different magnetic field intensity (MFI). It clearly observed that BN RMS and peak increased with increased magnetic field intensity at a constant magnetizing frequency (f_m) of 25 Hz, table feed rate of 9 m/min and downfeed of 40 µm. BN RMS and peak varied from 0.004-0.1 mV and 0.034-0.774 mV, respectively. Maximum RMS and peak values were obtained under an Al_2O_3 (1 wt.%) UVAMQL environment, which were higher, about 155-270% in RMS and 173-370% in peak than the RMS and peak values of dry grinding.

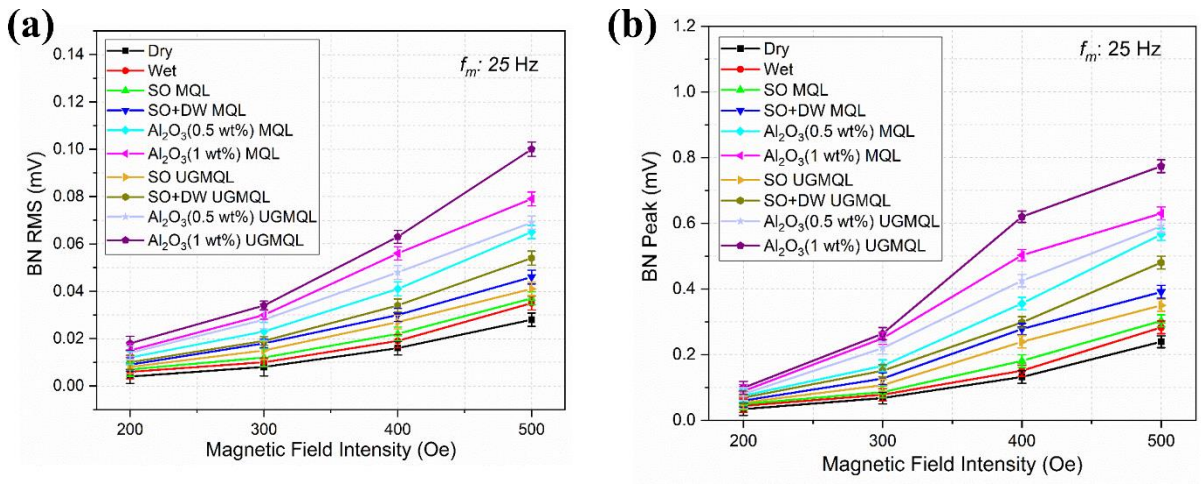

Figure 7.5 Variation in (a) RMS and, (b) peak, under different magnetic field intensity

RMS and peak values were found in dry, wet, SO MQL, SO+DW MQL, Al_2O_3 (0.5 wt.%) MQL, Al_2O_3 (1 wt.%) MQL, SO UVAMQL, SO+DW UVAMQL, Al_2O_3 (0.5 wt.%)

UVAMQL, Al_2O_3 (1 wt.%) UVAMQL about 0.028 and 0.239, 0.035 and 0.283, 0.037 and 0.303, 0.046 and 0.391, 0.065 and 0.566, 0.079 and 0.63, 0.041 and 0.35, 0.054 and 0.48, 0.069 and 0.591, and 0.1 and 0.774 mV, at MFI of 500 Oe, respectively.

Generally, effectiveness of MBN analysis depends upon the process parameters such as f_m and MFI. When the MFI was applied to the ground sample, the f_m of this field affects the penetration depth into the work material. As f_m increases, then decreases the depth penetration of the magnetic field, means low coverage of an area of penetration [286]. In other words, minimum subsurface was covered by a magnetic field at a higher frequency, resulting in a few grains boundary response to magnetic domain wall movement and overall pulse generation was infected. Shrivastava et al. [287] reported that the motion of domain walls becomes less due to thermal damage or plastic-deformed grain boundaries, which act as obstacles. Hence, poor BN responses in terms of lower RMS and peak value obtained.

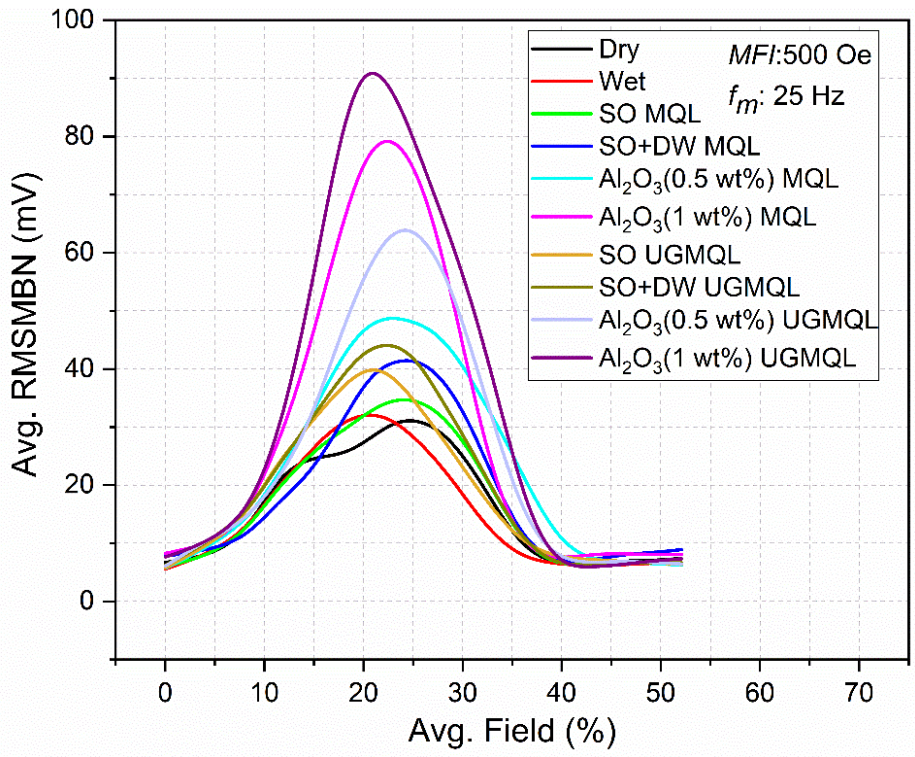

Figure 7.6 MBN envelope under different environmental conditions

On the other hand, magnetization energy was provided by an external magnetic field to the magnetic domain walls motion. More magnetic energy was developed with an increase MFI. An increase in MFI provides more acceleration for movement and rotation of magnetic domain walls. Apart from this, cooling and lubrication effects significantly influence the surface quality. By this effect, the occurrence of thermal damage over the surface was less due to their thermos-physical properties of lubricants, as discussed in Chapter 6.

Figure 7.6 shows the variation in the average envelope of the MBN signal under different grinding environments. A single peak MBN envelope was observed under each grinding environment after MBN analysis over the ground samples. This indicated no drastic microstructural changes to long depth occurred in the ground surface under different environments. Gurruchaga et al. [288] also reported a single peak MBN envelope. They investigated the effect of grain size on MBN envelope shape. As seen from Figure 7.6, the MBN envelope peak shifted towards higher field strength with low RMS amplitude under dry grinding than in other environments. This shift results from more severe thermal damage, which increases the number of grain boundaries and causes an increase in small grain size. Because these grain boundaries restrict the domain wall, stronger magnetic fields were needed to allow the domain wall to cross these pinning sites. Conversely, the MBN envelope under Al_2O_3 NFs-based grinding gets shifted towards the left side due to lower thermal damage than dry grinding. Furthermore, the shape of the MBN envelope changes with the increase in hardness, as shown in Figure 7.6.

7.2.4 Analysis of ground sample by magnetic HL parameters under different environments

Hysteresis loop study of the ground surfaces was carried out over a broad range of MFI (MFI: 200, 300, 400, and 500 Oe) with a constant f_m of 0.1 Hz and a wide range of f_m (f_m: 0.05, 0.1, 0.15, and 0.2 Hz) with a constant MFI of 450 Oe. The findings of the experiment showed that HL properties, such as permeability and coercivity, varied when ground samples were exposed to various temperatures. Figure 7.7 presents the changes in the permeability of ground samples under variable MFI and f_m conditions. Permeability is the ability of a ferromagnetic substrate to enable magnetic field generation. Figure 7.7 (a) shows the increasing trend of permeability with respect to MFI variation. Compared to grinding environments, minimum average permeability was found under dry grinding. In contrast, maximum permeability was obtained in Al_2O_3 NFs (1 wt.%) under UVAMQL grinding. These characteristics were reliant on the samples' hardness. Due to the strong magnetizing energy at high MFI, which assures good magnetization and leads to comparable behaviour in all samples, this occurred. Magnetic field also affect the magnetic tribology properties [289]. An increase in MFI raised the penetration depth of the magnetic field into the work material. Hence more volume of the material can get energized to cross the obstacles in the form of grain boundaries to achieve saturation. This causes the permeability of the ground sample to increase as a result.

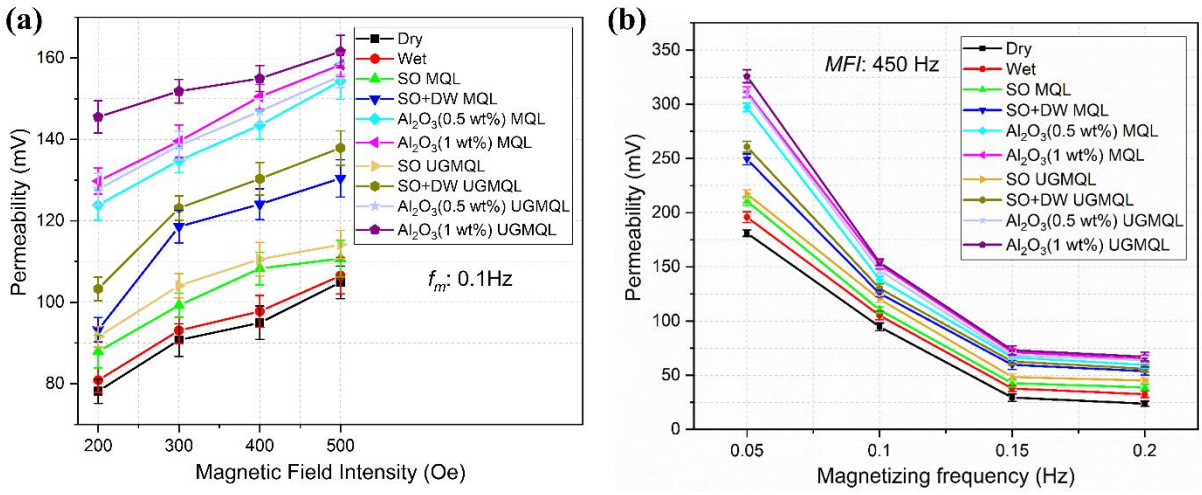

Figure 7.7 Permeability with MFI and f_m under different grinding environments

Figure 7.7 (b) indicates permeability decreases with an increase in f_m. The permeability value differs greatly between the low-frequency (0.05 Hz) and high-frequency (0.2 Hz). During UVAMQL grinding, a high permeability value was noted, approximately 331.58 at 0.05 Hz magnetizing frequency and 450 Oe MFI. But the low permeability value was recorded, about 72.28, under the magnetizing frequency of 0.2 Hz and MFI of 450 Oe. It depends on the hardness of the ground sample. Aside from that, when the magnetizing frequency is raised, the eddy current damping (i.e., reduction in the strength of the external magnetic field by eddy current) effect rises along with it, limiting the extent to which the magnetic field may penetrate the workpiece; less magnetic field penetration means fewer active domain walls, which in turn reduces the permeability during the HL process. A similar outcome was obtained by Awale et al. [265] when they investigated the effect of thermal damage on the surface integrity of work material AISI D2 tool steel using the HL technique. They also reported decreased permeability with an increase in the magnetizing frequency.

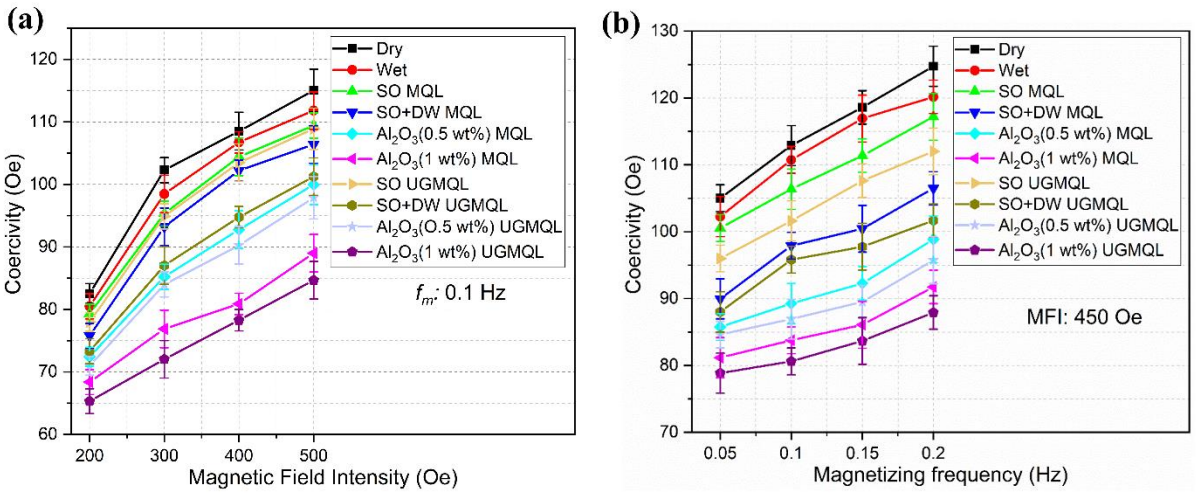

Figure 7.8 Coercivity with MFI and f_m under different grinding environments

Coercivity is the strength of the applied magnetic field needed to bring the material's magnetization to zero when the specimen's magnetization reaches saturation. It shows the resistivity of the ferromagnetic material to demagnetization. Coercivity is a promising parameter that varies with the material's characteristics, including hardness, stress, phase transformation, magnetizing frequency, and magnetic field intensity.

Figure 7.8 illustrates the variation in coercivity of the ground samples with MFI and f_m for different grinding environments. It indicated a significant increase in coercivity with an increase in the MFI and f_m (refer to Figure 7.8 (a) and (b)). Similar outcomes by Srivastava et al. [46] were reported on the pack carburised low carbon steel work material. Figure 7.8 reveals the increased coercivity with an increase in MFI. Increased MFI provides more magnetization energy. This energy accelerates magnetic domain wall motion to attain the saturation caused by the external magnetic field. Hence, greater strength of the reverse magnetic field is required after saturation to demagnetize the material. Severe thermal damage provided more hurdles for the magnetic domain wall motion. Therefore, the ground sample required a more energetic magnetic field to attain the saturation of the movement of the magnetic domain wall. This resulted in more coercivity of dry grinding compared to

the other environments. As the thermal damage surface decreased, lesser coercivity was noticed, as seen in Figure 7.8 (a). The coercivity of wet, SO MQL, SO+DW MQL, Al_2O_3 NFs (0.5 wt.%) MQL, Al_2O_3 NFs (1 wt.%) MQL, SO UVAMQL, SO+DW UVAMQL, Al_2O_3 NFs (0.5 wt.%) UVAMQL, Al_2O_3 NFs (1 wt.%) UVAMQL at higher MFI were 111.81, 109.4, 106.38, 99.95, 88.98, 108.89, 101.24, 97.87, and 84.66 Oe, respectively, which were reduced by 2.78%, 4.88%, 8.37%, 12.23%, 22.63%, 6.21%, 11.10%, 14.90%, and 26.39%, respectively, relative to that of dry environment.

Figure 7.8 (b) depicts the variation in coercivity with increased f_m for the ground samples under various environments. A rise in f_m reduces the amount of magnetic field penetration into the material, which corresponds to an increase in the reverse MFI required to cause the magnetization to zero after saturation (called coercivity). As a result, coercivity rises as f_m rises. Further, the grain refinement and increased hardness upon dry grinding resulted in the formation of more hurdles in the form of more grain boundaries. The magnetic domain wall movement becomes challenging, resulting in the allowance of less penetration of the magnetic field into the ground samples of dry grinding. Thus, the coercivity value was consistently higher in the case of the dry grinding sample in comparison to the remaining grinding environment samples. Also, increased plastic deformation in the sub-layer of the ground surface resulted in an increase in the coercivity of the ground samples [290]. The results of the analysis of ten ground samples indicated that there was a significant relationship between the coercivity value and the level of thermal damage. Specifically, as the thermal damage increased, the coercivity value also increased. The lower coercivity was obtained in the Al_2O_3 NFs (1 wt.%) under UVAMQL grinding owing to negligible phase transformation in the work material.

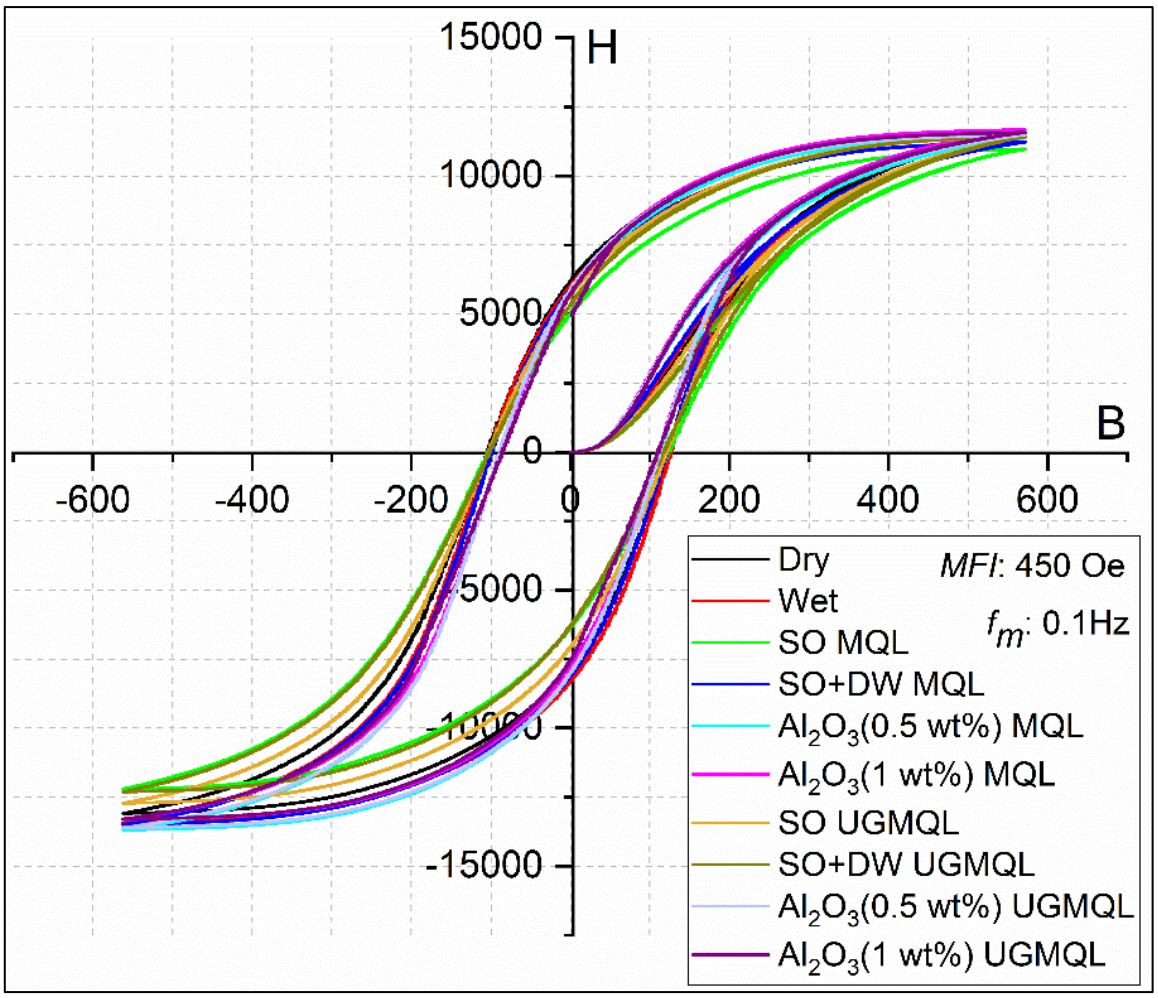

Figure 7.9 Hysteresis loop envelope under different environmental conditions

The hysteresis loop describes the material behaviour during magnetization and demagnetization. The hysteresis curve is drawn between magnetic flux density (B) and magnetizing force (H), as depicted in Figure 7.9. The change in material properties of ground samples during various grinding environments also affected the shape of the hysteresis loop. After applying an external magnetic field to a ferromagnetic material with zero initial magnetic flux density, i.e., negligible magnetic property, the majority of magnetic domains aligned with the direction of the external magnetic field, while some magnetic domains aligned with the opposite direction. The magnetic field intensity exhibited a distinct path from its initial value of zero up to the point of saturation. Moreover,

it should be noted that an increase in the external magnetic field does not result in a corresponding increase in magnetic flux density. It is observed that magnetized materials exhibit a deviation from their original path during the process of demagnetization. The region encompassing the processes of magnetization and demagnetization is commonly referred to as the hysteresis loop, which is characterized by a significant loss of energy in a single cycle. Typically, the thermal degradation of ground samples can result in distinct variations in the shape of the hysteresis loop, which can be attributed to the magnetic domain wall motion. Moreover, a shorter and wider hysteresis loop can be achieved for a ground sample with higher hardness due to the presence of a greater number of obstacles that impede the movement of domain walls.

Figure 7.9 illustrates the hysteresis loop envelope of ground samples at MFI of 450 Oe and f_m of 0.1 Hz under different grinding environments. In the present work, as seen in Figure 7.9, Al_2O_3 nanofluid with 1 wt.% concentration under UVAMQL grinding has a long and thin shape of hysteresis loop. It was mainly due to the slightly highest magnetization and demagnetization saturation point while applying the same magnetic field to ground samples. The saturated magnetic flux density was high for it, indicating that this ground sample got more magnetized, followed by the remaining samples under different environments because of its low hardness and less energy loss during the single cycle. As hardness increased, the hysteresis loop changed, resulting in a small and thick shape. Diwakar et al. [291] studied the hysteresis loop analysis on IS 2062 steel and AISI D2 tool steel work material. They reported a change in the shape of the hysteresis loop. Higher hardness material, i.e., AISI D2 tool steel, compared to lower hardness material like IS 2062 steel, has a short and thick shape of the hysteresis loop.

7.3 Conclusion

Following conclusions may be drawn from the present experimental study:

- Maximum microhardness variation and thermal damage layer (dark zone) were observed in the case of dry grinding due to a huge amount of heat generation at the grinding zone.
- According to MBN outcomes, a higher RMS and peak were observed in the UVAMQL-NFs ground sample due to the lower hardness, which helps in magnetic domain walls movement.
- According to HL analysis, maximum permeability and minimum coercivity were obtained in the UVAMQL-NFs based sample due to easier domain wall movement in the ground sample.
- MBN and HL envelopes shrink with a decrease in microhardness under all grinding modes. MBN envelope was shifted towards lower magnetic field strength due to minimum obstacle in domain wall displacement.